3-29-2012

Low-loss Meta-atom for Improved Resonance Response

Derrick Langley

Ronald Coutu Jr.
Air Force Institute of Technology

Peter J. Collins
Air Force Institute of Technology

Recommended Citation

Langley, D., Coutu, R. A., & Collins, P. J. (2012). Low-loss meta-atom for improved resonance response. AIP Advances, 2(1), 012196. https://doi.org/10.1063/1.3701709

Low-loss meta-atom for improved resonance response

Cite as: AIP Advances **2**, 012196 (2012); https://doi.org/10.1063/1.3701709
Submitted: 20 October 2011 . Accepted: 08 February 2012 . Published Online: 29 March 2012

Derrick Langley, Ronald A. Coutu, and Peter J. Collins

Low-loss meta-atom for improved resonance response

Derrick Langley,[a] Ronald A. Coutu, Jr., and Peter J. Collins
Department of Electrical and Computer Engineering, Air Force Institute of Technology, 2950 Hobson Way, Bldg 641, Wright-Patterson AFB Ohio, 45433, USA

(Received 20 October 2011; accepted 8 February 2012; published online 29 March 2012)

Measurements of a meta-atom integrated with a low noise amplifier into the split-ring resonator are presented. A comparison is made between baseline meta-atoms and one integrated with a GaAs low noise amplifier. S-parameter measurements in a RF strip-line show the resonant frequency location. The resonance null is more prominent for the integrated meta-atom. Biasing the low noise amplifier from 0 to 7 VDC showed that the resonant null improved with biasing voltage. As the biasing voltage increases, the transmission null reduced from -11.82 to -23.21 dB for biases from 0 to 7 VDC at resonant frequency. *This is a work of the U.S. Government and is not subject to copyright protection in the United States.* [http://dx.doi.org/10.1063/1.3701709]

A meta-atom is the building block for metamaterials. Metamaterials are bulk structures that effect the propagation of electromagnetic waves by effectively altering the signal at a specific frequency. The first split ring resonator was constructed by Pendry *et al.* who describe metamaterials as a structure that determines the effective permittivity and permeability through engineered materials.[1,2] Based on his research, others have made advances to the study of metamaterials across the electromagnetic spectrum.[3–6] In,[7] Hand and Cummer use barium strontium titanate thin film capacitors as external components to shift the resonant frequency. For an application example, an invisibility cloak at radio frequencies (RF) diverts signals around an object rendering it undetectable.[8] In,[9] Chen *et al.* constructed active terahertz (THz) metamaterial devices which modulated the transmission. An approach to reduce loss with gain medium was demonstrated by Yuan *et al.* using a RF amplifier and phase shifter at megahertz frequencies.[10] Using a dye of Rh800-epoxy, Xiao *et al.* developed a loss-free and active metamaterial at optical frequencies.[11] Another example of using gain was demonstrated by Casares-Miranda *et al.* with a high-gain active composite right/left handed leaky wave antenna using amplifiers along the metamaterial structure.[12] Popov and Shalaev showed the feasibility of compensating losses in metamaterials by optical parametric amplification.[13] Ramakrishna and Pendry show gain at optical frequencies is possible with layers of silver and a positive amplifying dielectric medium.[14] Jiang *et al.* recently demonstrated an active microwave negative index metamaterial transmission line (not an individual meta-atom) with germanium tunnel diode as the gain element inserted in the transmission line.[15] Finally, Kozyrev *et al.* demonstrated the left handed nonlinear transmission line media with gain as an alternative to negative index media.[16]

The effective parameters for the meta-atom are capacitance and induction. Capacitance (C) helps to establish the effective permittivity. Inductance (L) helps to determine the magnetic permeability for the structure. Combining the effective parameters into the resonant frequency produces a resonant LC response not found in natural materials. The effective permittivity and permeability determine the refractive index of the meta-atom and can be used to understand the behavior of metamaterials at a given frequency.[4] Knowing metamaterials behavior can lead to the design of components for radar applications, sub-wavelength imagery systems and cloaking.

In this investigation, a low noise amplifier (LNA) integrated in the meta-atom is constructed to compensate the loss in meta-atoms. The LNA is integrated into the split ring resonator is a novel

[a]Author to whom correspondence should be addressed. Electronic mail: Derrick.Langley@afit.edu

approach to implement low loss meta-atoms at gigahertz frequencies. By inserting a gain medium into the baseline split ring resonator, the current flow, and charge density is affected around the split ring resonator.

Meta-atoms effect propagating signals to the point where a desirable resonant frequency is established from material properties and structural dimensions. At the resonant frequency, split ring resonators significantly reduce the signal transmission. At the RF frequencies, the resonance equation

$$\omega_{res} = \frac{1}{\sqrt{2\pi(L_{Outer} + L_{Inner})_{Avg}(C_{Outer} + C_{Inner} + C_{Left\_Trace} + C_{Right\_Trace})}} \tag{1}$$

involves average inductance and total capacitance parameters from the split ring resonator consisting of inner and outer split rings.

Based on the resonant frequency, the effective magnetic permeability model

$$\mu(\omega) = 1 + \frac{f\omega^2}{\omega_{res}^2 - \omega^2 - i\Gamma\omega}, \tag{2}$$

describes the behavior for split ring resonator meta-atoms where the fill factor (f) and damping factor (Γ) are associated with material losses. The fill factor depends on feature dimensions and periodic spacing by $f = \pi l^2/4a^2$. The damping factor is dependent on the material resistivity of the split ring by $\Gamma = (4\rho)/(\mu_0)$.

The capacitance for the resonant frequency is determined by considering the capacitance between the inner and outer ring, capacitance at the gap of each ring and capacitance for each trace. Using the parallel plate capacitance model,

$$C = \varepsilon_r \varepsilon_0 \frac{A}{gap} \tag{3}$$

the capacitance can be calculated with this analytic model. To solve more complicated structures, finite element methods (FEM) are used to determine the capacitance on each element node. With the capacitance model, the relative permittivity (ε_r), dimensions for capacitance area (A) and separation gap (gap) all contribute to the overall capacitance of the structure. By manipulating these parameters, the capacitance of each meta-atom can be established resulting in a fixed resonant frequency.

The inductance depends on the metal, length, width and total induced current on the split ring resonator. Inductance is defined as

$$L = \frac{\psi_{ij}}{I_j} \quad \text{for } I_k = 0 \text{ if } k \neq j, \tag{4}$$

where ψ_{ij} represents the magnetic flux in the ring due to a current I_j in the ring j.[17] From this definition, the self-inductance of the split ring resonator can be described using the dimensions of the structure and the induced current. Tracing the current path around the split ring resonator after a potential is placed across the gap allows the calculation of the self induction. Figure 1(a) shows the *LC* resonator circuit that describes the operation of the meta-atom as an equivalent circuit model. The current path around the split ring controls the charge built up. By controlling the amount of charge density around the meta-atom, the low noise amplifier inserted in the current path helps minimize loss.

For the research into the active element, a 0.5 – 6.0 GHz Low Noise Gallium Arsenide (GaAs) MMIC Amplifier is chosen as the gain medium integrated into the outer split ring resonator.[18] A 1 – 4 GHz baseline meta-atom design is chosen to integrate the active element because of the size, ease of device integration and available LNAs operating at the 1 – 4 GHz frequency range. Figure 1(b) shows the equivalent circuit for the LNA which uses PHEMT technology with self-biasing current sources, a source-follower inter-stage, resistive feedback, and on-chip impedance matching networks. The normal operating voltage range of the amplifier is 0 – 7 VDC and generates 18 – 20 dB of gain at ~4 GHz. The concept behind the integration is to have the ability to enhance current flow around the SRR. The current flow for the outer split ring resonator travels from the large split ring resonator gap around the ring to the RF input of the amplifier. The current flow then proceeds out of the amplifier

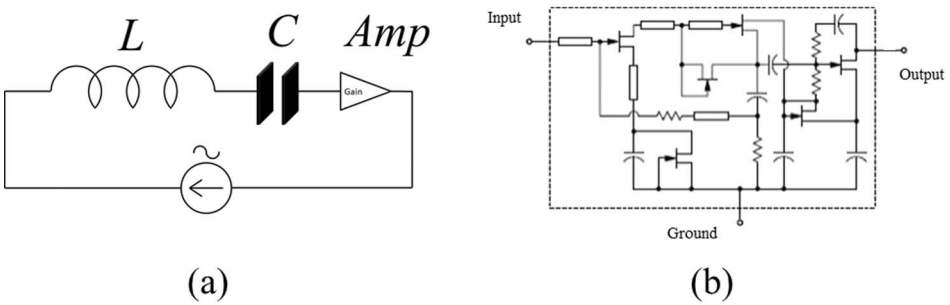

FIG. 1. a) *LC* resonator model integrated with gain element. b) Equivalent Circuit of the Avago Technologies MGA-86563 GaAs MMIC low noise amplifier (Avago Technologies MGA-86563 - 0.5–6 GHz Low Noise GaAs MMIC Amplifier datasheet, Web link: http//avagotech.com/docs/AV02-2514EN, Publication number: AV02-2514EN).[18]

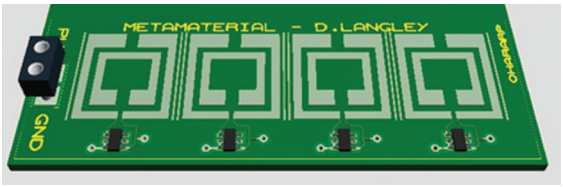

FIG. 2. Active element integrated into the 1 – 4 GHz meta-atom. The low noise GaAs amplifier integrated into the baseline meta-atom effects the resonant frequency based on a gain medium inserted into the outer SRR.

and continues around the split ring resonator stopping at the opposite side of the large gap. The large gap of the split ring resonator functions as a charged capacitor generating the electromagnetic field that provides a charge built up on the split ring resonator. The low noise amplifier controls the amount of free flowing electrons traveling through the split ring which in turns controls the resonance of the meta-atom to counter act any loss.

Figure 2 shows the layout consisting of the 1 – 4 GHz baseline meta-atom along with the LNA placed on landing pads for surface mount devices, and interconnects for DC bias and ground. A 0.40 mm gap was cut out of the outer split ring resonator to integrate the LNA and interconnects. The DC bias and ground interconnect traces are located on the backside of the layout and connected with thru-vias to the topside for the LNA. The design layouts are inspected and sent for fabrication on double sided printed circuit board made of insulating glass reinforced epoxy resin (FR4) at a commercial foundry.[19]

Simulations of the meta-atom were completed using CoventorWare® to obtain the capacitance and induction values for the split ring resonators and metal traces.[20] The metal structures were simulated with copper. The capacitance values for the meta-atom design are 0.327 pF and 0.675 pF for the inner and outer split rings, respectively. Each metal trace provides a capacitance of 0.160 pF to the design. The inductance values for the design are 8.86 nanoHenry (nH) for the inner split ring resonator. The outer split ring resonator is divided into two sections with a 0.4 mm gap and each provides 9.16 nH to the design. Based on these values, the resonant frequency is 3.64 GHz. The design is simulated without the gap in the outer ring and the resonant frequency is estimated to be 2.79 GHz. This provides a possible 0.85 GHz range for the resonant frequency location with the LNA providing the channel for current flow.

Two samples of the 1 × 4 array of the meta-atom design were placed between the inner and outer conductor of a 4 GHz RF strip-line as shown in Figure 3(a). The meta-atom arrays are inserted into the strip-line oriented normal to the transverse electromagnetic mode for RF testing. An Agilent Technologies E8362B programmable network analyzer stimulates and measures the RF signal. S-parameters within the 10 MHz to 4 GHz range incident on the meta-atom arrays are collected for analysis.

The resonance frequency appears at 3.85 GHz slightly higher than the simulated values. Integrating the LNA into the split ring resonator increased the resonant null for the meta-atom, but is based on

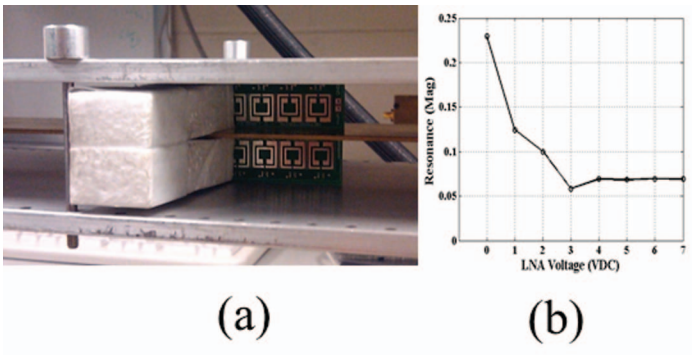

FIG. 3. a) Meta-atom array placed in 4 GHz RF strip-line. b) Meta-atom resonant null as a function of applied bias.

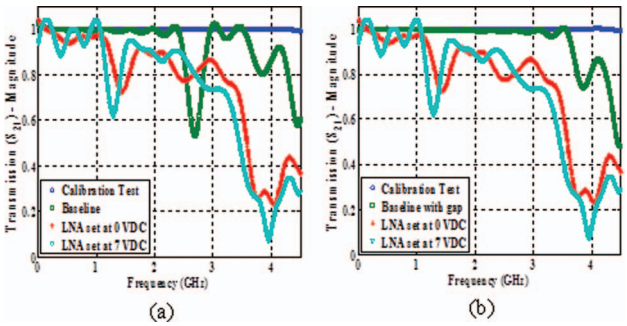

FIG. 4. a) Baseline (green) and Integrated Meta-atom transmission response (red, blue), b) Baseline with gap (green) and Integrated Meta-atom (red, blue) transmission responses to the designs inserted in the RF Strip-line.

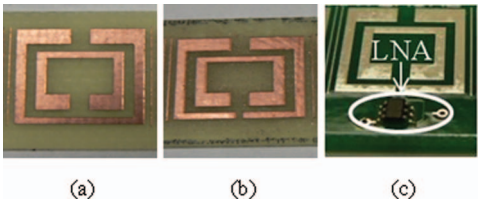

FIG. 5. a) Baseline, b) Baseline with gap and c) Meta-atom integrated with a LNA.

the amount of biasing voltage applied. For comparison, a 1 – 4 GHz Baseline sample without a gain medium is tested to see how the resonance null compares to the meta-atom integrated with the LNA. The resonant frequency for the Baseline sample appears at 2.69 GHz and reduced to -5.51 dB. As another comparison, samples were made with a gap in the Baseline outer split ring resonator. Test results for this sample shows a resonance at 3.86 GHz with a -2.61 dB null. The integrated samples were biased from 0 to 7 VDC and changed the resonant null based on the bias voltage. Figure 3(b) shows the magnitude of the resonant null experimental results as the bias voltage increased. At 5 VDC, the LNA reaches its peak operational gain of 18.8 dB while at 4 GHz. These experimental results match the simulation results for the *LC* resonant circuit at the resonant frequency location and expected null. With the amplifier turned off (0VDC), the resonant frequency appears at 3.75 GHz with a reduction in the transmission to -11.82 dB. As the biasing voltage increases, the resonant frequency shifts to as much as 3.95 GHz with transmission reduced to -23.21 dB when biased at 7.0 VDC. Figure 4(a) and 4(b) show the transmission data plotted for the meta-atoms over the 10 MHz to 4.2 GHz range. Figure 5 shows the designs used for experimental testing.

Integrating the meta-atom with a low noise amplifier has improved the null at the resonant frequency. These experimental results demonstrate that the level of the resonant null can be controlled with a gain medium to compensate for loss. The lowest transmission level (-23.21 dB) occurs while

the LNA is biased (7 VDC). This research shows that a gain medium such as the LNA can improve the null at the resonant frequency.

ACKNOWLEDGMENTS

The financial support and sponsorship of this project were provided by Drs. Katie Thorp and Augustine Urbas from the Air Force Research Laboratory (AFRL), Materials and Manufacturing Directorate. The authors are also thankful to Ryan O'Hara for advice on printed circuit board layouts as well as AFIT clean room support from Rick Patton and Rich Johnston.

Disclaimer: The views expressed in this article are those of the authors and do not reflect the official policy or positions of the United States Air Force, Department of Defense, or the U. S. Government.

[1] J. B. Pendry, A. J. Holden, D. J. Robbins, and W. J. Stewart, IEEE Transactions on Microwave Theory & Techniques **47**, 11 (1999).
[2] J. B. Pendry, Physical Review Letters **85**, 18 (2000).
[3] D. R. Smith, W. J. Padilla, D. C. Vier, S. C. Nemat-Nasser, and S. Schultz, Physical Review Letters **84**, 18 (2000).
[4] D. R. Smith, S. Schultz, P. Markos, and C. M. Soukoulis, Physical Review B **65**, 195104 (2002).
[5] B. Popa and S. A. Cummer, Microwave and Optical Technology Letters **49**, 10 (2007).
[6] D. Huang, E. Poutrina, and D. R. Smith, Applied Physics Letters **96**, 104104 (2010).
[7] T. H. Hand and S. A. Cummer, Journal of Applied Physics **103**, 066105 (2008).
[8] D. Schuring, J. J. Mock, B. J. Justice, S. A. Cummer, J. B. Pendry, A. F. Starr, and D. R. Smith, Science **314**, 5801 (2006).
[9] H. Chen, W. J. Padilla, J. M. O. Zide, A. C. Gossard, A. J. Taylor, and R. D. Averitt, Nature **444** (2006).
[10] Y. Yuan, B. Popa, and S. A. Cummer, Optics Express **17**, 18 (2009).
[11] S. Xiao, V. P. Drachev, A. V. Kildishev, X. Ni, U. K. Chettiar, H. Yuan, and V. M. Shalaev, Nature **466** (2010).
[12] F. P. Casares-Miranda, C. Camacho-Peñalosa, and C. Caloz, IEEE Transactions on Antennas and Propagation **45**, 8 (2006).
[13] A. K. Popov and V. M. Shalaev, Optics Letters **31**, 14 (2006).
[14] S. A. Ramakrishna and J. B. Pendry, Physical Review B **67**, 201101 (2003).
[15] T. Jiang, K. Chang, L. Si, L. Ran, and H. Xin, Physical Review Letters **107**, 205503 (2011).
[16] A. B. Kozyrev, H. Kim, and D. W. van der Weide, Applied Physics Letters **88**, 264101 (2006).
[17] E. A. Ruehli, IBM Journal Research and Development **16**, 5 (1972).
[18] Avago Technologies MGA-86563 - 0.5–6 GHz Low Noise GaAs MMIC Amplifier Datasheet, Web link: http://www.avagotech.com/docs/AV02-2514EN, Publication number: AV02-2514EN.
[19] Advanced Circuits: http://www.4pcb.com.
[20] CoventorWare® is a resistered trademark of Coventor, Inc.: http://www.coventor.com/coventorware.html.